28th HENAAC Conference
Research Posters Competition
Winners

Anaheim, CA

October 5 – 9, 2016

FIRST PLACE UNDERGRADUATE – SCIENCE/MATH

Understanding Growth Behavior of Alumina (Al_2O_3) Nanoparticles

M. R. Casillas, F. A. Fasulo, N. S. Bell, T. J. Boyle, L. J. Treadwell, and B. A. Hernandez-Sanchez
Sandia National Laboratories, Advanced Materials Laboratory, 1001 University Blvd., SE
Albuquerque, NM 87106

Keywords: alumina, nanoparticles, precursor effect, solution processing, nano inks

Alumina (Al_2O_3 or aluminum oxide) is an important metal oxide used in variety of applications due to its chemical and thermal stability. Both bulk and nanoscale powders can be found in numerous commercial products such as sunscreens, cosmetics, electronics, and paints. In addition to being useful as a catalyst and support, Al_2O_3 has been an integral ink material used in direct write (robocasting) processes. Critical to these applications is understanding how Al_2O_3 crystals grow under various processing conditions in order to control its properties.

Al_2O_3 is a naturally occurring crystalline mineral which can adopt seven different crystalline phases. Alpha-alumina, or corundum, is the most common phase found and used. The α-Al_2O_3 phase crystallizes as a hexagonal scalenoheral structure where aluminum cations occupy 2/3 of the octahedral sites among the hexagonal closed-packed oxygen anions. Bulk materials have been synthesized through solid state, spray-dry, and sol-gel reaction routes which all require extremely high temperatures and/or pressures to obtain the alpha phase. Recently, α-Al_2O_3 nanoparticles were synthesized by solution combustion synthesis and sol-gel processing using aluminum nitrate, -halide, -hydroxide, and –alkoxide precursors. Through these investigations, various sizes and shapes have been isolated and results indicate that the aluminum precursor or solvents used may influence particle shape.

In order to understand growth behavior of Al_2O_3 nanoparticles, the effect of precursor on nanoparticle phase and morphology was examined within solution processing routes. Solution nanoparticle processing routes (e.g., glycothermal, solvothermal, and solution precipitation) were used to lower the temperatures and/or pressures required to reach the α-Al_2O_3 . The following aluminum precursors were evaluated under solution nanoparticle processing routes: aluminum isopropoxide ($Al(OPr^i)_3$), gibbsite ($Al(OH)_3$), and boehmite ($AlO(OH)$). These were selected for their previous production of phase pure bulk alumina in sol-gel and solid state reactions.

First, glycothermal synthesis of alumina using a bench top reactor under an inert atmosphere was conducted. Particles are generated form commercially available gibbsite reacted with Al_2O_3 nano seeds in 1,4-butanediol ($C_4H_{10}O_2$).[1] Nano alumina and boehmite seeds were used as an additive to determine their influence on final phase and yield. The seeds provide a nucleation site for the nano alumina particles to grow from. To take advantage of alumina's solubility curve, another variable, potassium hydroxide (KOH) was also explored as an additive to determine if a greater percent yield of the particles could be obtained by adjusting the pH of the solution.

Next, alumina synthesized through solution precipitation synthesis was performed using the same precursors, solvents and additives found in the glycothermal route. The difference in

processing employed refluxing the solutions under ambient conditions as opposed to high pressure. Finally, alumina can be produced from beohmite. This requires the synthesis of nanoscaled boehmite followed by heat treatment of these powders. These boehmite particles were produced through solvothermal and solution precipitation synthesis. Commercially available aluminum isopropoxide, aluminum hydroxide, and aluminum nitrate nonahydrate were evalutate as precursors to change the morphology of boehmite. rods, rectangular platelets, and stacked platelets were synthesized using these methods.

To determine the precursor effect, all the resulting particle morphology and sizes were characterized by Scanning Electron Microscopy (SEM), Transmission Electron Microscopy (TEM), and Dynamic Light Scattering (DLS). The particle phase was identified with Powder X-ray Diffraction (PXRD). The results indicate that precursor and synthesis route impacts the morphology and phase of alumina.

For Glycothermal, Alpha-alumina particles were produced; however, the particle sizes were much larger than expected. Future research will be conducted to reduce the size of the particles produced by rotor milling and ultra-sonicating the particles. Heat treatment of boehmite prepared by solovthermal and solution precipation resulted in platelets with a similar crystal structure of commercially available nano alumina. The synthesis of boehmite also showed that using aluminum hydroxide resulted in rod shaped particles, whereas aluminum isopropoxide resulted in platelet shaped particles. Full details on characterization and synthesis will be presented.

This work was supported in part by Laboratory Directed Research and Development (LDRD), Department of Energy (DOE), Geothermal Technologies Office (GTO) under the Office of Energy Efficiency and Renewable Energy (EERE), and by the Sandia STAR Program. Sandia National Laboratories, a multi-program laboratory managed and operated by Sandia Corporation, a wholly owned subsidiary of Lockheed Martin Corporation, for the U.S. Department of Energy's National Nuclear Security Administration under contract DE-AC04-94AL85000.

Reference:

1. Nelson S. Bell., Seung-Beom Cho, and James H. Adair. "High-Temperature Synthesis of Materials: Glycothermal Synthesis of Alpha Aluminum Oxide." Synthesis and Characterization of Advanced Materials ACS Symposium Series 681 (1997): 120-33. Web.

SECOND PLACE UNDERGRADUATE – SCIENCE/MATH

Chemistries for Tumor Cell Detection

J.V. Guerrero, I. Fernandez, M.K. Rahim, and J.B. Haun
University of California, Irvine, Irvine, CA 92697

Keywords: bioorthogonal chemistry, Diels-Alder cycloaddition, dienophile, molecular imaging, tumor detection

Reliable imaging methods are crucial for accurate cancer detection, diagnosis, approach for treatment and overall mortality rate. Most cancer cells possess differential biomarker concentrations compared to healthy human cells, contributing to the tumor's ability to grow. The difference in biomarker expression can be leveraged to improve distinction between cancer cells and healthy cells. Furthermore, conducting molecular imaging through two-step pre-targeting methods improves the signal-to-noise ratio when imaging tumors, allowing for more accurate diagnosis. Owing to the relatively small size of the molecules and fast reaction speeds, bioorthogonal chemistries enhance this pre-targeting strategy by maximizing the selectivity of affinity molecule and imaging agent. However, previous work demonstrated that bioconjugation between antibodies and TCO (*trans*-cyclooctene) dienophile via amine-reactive NHS (*N*-hydroxysuccinimide) resulted in overall low yields in TCO functionality, presumably because TCOs are enveloped in hydrophobic pockets of the antibody. Alternatively, attaching TCO to antibodies via DBCO-PEG-TCO (dibenzylcyclooctyne-polyethylene glycol- *trans*-cyclooctene) linkers result in fully functional TCOs. Strained-ring dienophiles, such as these TCOs, are commonly used in bioorthogonal pre-targeting methods because of their high reactivity rates. However, alternative dienophiles are also of interest due to their unique range of properties, such as chemical stability and size.

In this study, we investigate whether other strained-ring dienophiles exhibit the same low functionality when attached directly to Herceptin antibody and also explore potential contributing factors. The dienophiles of interest for the study include norbornene, cyclopropene, dibenzylcyclooctyne (DBCO) & bicyclo[6.1.0]nonyne (BCN). Finally, we plan to restore functionality of these dienophiles using linkers that were previously proved to be successful with TCO.

Dienophile conjugates are prepared by reacting 250 μg of Herceptin antibody with 10, 20, 30 equivalents of one of several amine-reactive dienophile linkers in 0.2 mL PBS containing 0.1 M $NaHCO_3$ (pH 8.5). Total dienophile densities are determined based on changes in mass using matrix assisted laser desorption/ionization – time of flight (MALDI-TOF) mass spectrometry. Functional dienophile loadings are measured by reaction of 100 μg dienophile-modified antibodies with 200 μM tetrazine–Oregon Green dye. In order to quantify the total amount of fluorophores per antibody, absorption measurements are performed using a UV-Vis Spectrophotometer.

Herceptin antibodies were modified directly with norbornene, cyclopropene, DBCO or BCN strained-ring dienophiles via amine-reactive NHS chemistry. The preliminary results showed that NHS-BCN exhibited the greatest functionality with 60%. The remaining three dienophiles

exhibited less than 20% functionality. These results prove that the majority of the total antibody modifications were not reactive. Cyclopropene dienophile exhibited 20% functionality, becoming the second highest from the samples. Cyclopropene was followed by norbornene with 16%. Lastly, DBCO presented 5% functionality, the lowest of all four dienophiles tested. Reaction time and dye availability were not considered as limiting factors. Reaction time was not limiting because the reaction had an extended time period to be carried out. The presence of dye in the reaction was in excess quantities, dismissing the probability that it was limiting. We hypothesize that the chemical properties of the dienophiles involved in the experiment contributed to the degrees of varying functionality. This is probable because improves with relative hydrophilicity. Additional experiments were conducted with NHS-PEG-DBCO and NHS-PEG-norbornene, and these resulted in 3% and 25% functionality, respectively. This supports previously stated results in the work involving TCOs where it was demonstrated that functionality was improved while PEG was present to decrease the influences of hydrophobic pockets within the structure.

Future work involves experiments that will help identify the contributing factors that cause the decreased functionality of dienophiles. Further investigation will focus on the use of these strained-ring dienophiles in a two-step method to observe whether or not functionality is restored and to what percentage of functionality can be achiev

THIRD PLACE UNDERGRADUATE – MATH/SCIENCE

Gingivitis Prevention: Integration of Iron (II, III) Oxide Nanoparticles into Commercial Mouthwash

J. Nguyen and M. Osinski
University of New Mexico, Albuquerque, NM 87120

Keywords: gingivitis, periodontal disease, nanoparticles, iron oxide, mouthwash

Data from the Center for Disease Control and Prevention estimated that 64.7 million of American adults are victims of periodontitis, a dangerous and irreversible periodontal disease. The early form of periodontitis is gingivitis, a reversible, yet widespread disease, that is commonly overlooked. Therefore, the field of nanoscience has undertaken the unchartered task to incorporate nanoparticles into dental care. Nanoparticles have outstanding antimicrobial abilities, but nanoparticles in high concentrations may cause cytotoxicity and inflammation within the human body. Currently, the prescribed treatment for gingivitis is inadequate and depends on increased vigilance towards household dental care. The poor quality of gingivitis treatment and the biomedical limitations of nanoparticles have led to the need for the development of non-toxic substances that have increased potency as an antimicrobial, but are safe enough to be used in dental care products.

We hypothesize that biodegradable iron (II, III) oxide (Fe_3O_4) nanoparticles dispersed in Listerine Coolmint mouthwash may prevent the onset of gingivitis while reducing the time required to be spent on daily oral hygiene, making dental care more efficient and appealing for many gingivitis patients. Fe_3O_4 nanoparticles are FDA approved and are proven, with previous studies conducted with cystic fibrosis, to be miniscule enough, with an average diameter of 5 nm, to penetrate thick bacterial biofilm and administer medication directly to the bacteria colony. We predict that this same mechanism can be applied to gingiva bacterial biofilm, with Listerine Coolmint mouthwash as the main antiseptic. If the antibacterial strength of the mouthwash can be increased due to the incorporation of Fe_3O_4 nanoparticles, it is possible that the time needed to rinse with the mouthwash may be decreased from the recommended minimum of 30 seconds.

To evaluate our hypothesis, we synthesized Fe_3O_4 nanoparticles using iron acetylacetonate ($Fe(acac)_3$) as our precursor. $Fe(acac)_3$ was dissolved in an organic solvent, triethylene glycol (TREG), which does not stimulate the immune system and makes the nanoparticles water-soluble. After the synthesis, the nanoparticles were subject to ultrasound sonication and washing in acetone. The superparamagnetic nanoparticles were then extracted from the acetone, via arc magnets, and were further diluted in deionized water. We varied the concentration of the nanoparticles from 7 mg/mL (milligrams of nanoparticles per milliliter of water) to $2x10^{-2}$ mg/mL to $2x10^{-8}$ mg/mL. These concentrations served as milestones to determine the appropriate concentration for nanoparticle-characterization purposes in water and then in Listerine Coolmint mouthwash.

We found that the nanoparticle synthesis was very efficient as it produced a 93% yield. Furthermore, four characterization methods using dynamic light scattering (DLS), zeta potential,

transmission electron microscopy (TEM), and spectrophotometry measurements were utilized. 1) The DLS graph of the nanoparticles' radii versus the number of measurement counts confirmed that the average radius of one nanoparticle spans approximately 5 nm, which is consistent with the same nanoparticles used in the cystic fibrosis experiment. 2) The zeta potential of the nanoparticles was measured to be -22.3 mV, which is outside of the colloidal instability range of -20 to 20 mV. This signifies that the nanoparticles have a high colloidal stability in water and may potentially have a long shelf life when dispersed in Listerine Coolmint mouthwash. 3) The TEM images showed that the nanoparticles have a uniform size and shape distribution and further confirms the Fe_3O_4 composition of the particles. 4) Lastly, the spectrophotometry spectra showed that the nanoparticles have high absorptions within the ultraviolet and visible wavelength range, which is confirmed by the nanoparticles' black color.

Further progress in our methods will require us to receive approval from the Institutional Review Board to obtain gingival swabs from gingivitis patients. The mixed culture bacteria from these swabs will further be propagated using agar on disks of hydroxyapatite (a prominent mineral found in human teeth). A series of matrix studies will be conducted with two control groups and an experimental group. All groups will be subject to the same environment on an orbital shaker (to simulate rinsing motions) in an incubator at human body temperature (36.5 – 37.2 ^{o}C). The first control group will contain gingival bacteria subject to no treatment, the second control group will involve exposing gingival bacteria to plain Listerine Coolmint mouthwash, and the experimental group will include various concentrations of nanoparticles in mouthwash applied to gingival bacteria. Each group will be examined after increments of 10, 30, and 60 seconds. The viability of the gingival biofilm will be examined using the LIVE/DEAD BacLight Bacterial Viability Kit and cell culture size counting.

The characterization data from the Fe_3O_4 nanoparticles and the literature suggest that the nanoparticles may be highly effective as a biomedically innocuous antimicrobial that, when combined with Listerine Coolmint Mouthwash, can increase the potency of the mouthwash. This creates a promising dental care treatment that can be easily incorporated into routine dental hygiene practices to effectively prevent the onset of gingivitis.

FIRST PLACE UNDERGRADUATE – ENGINEERING/TECHNOLOGY

Single Board Computer, High-Resolution Micro Endoscope for Point of Care Cancer Detection (PI-HRME)

G. F. Lopez[1], S. Parra[2] and R. Richards-Kortum[2]
[1]University of Texas Rio Grande Valley, Edinburg, TX 78539
[2]Department of Bioengineering, Rice University, Houston, TX 77005

Keywords: Cancer, Cervical Cancer, Bioengineering, Cell imaging, Microcontrollers

Unfortunately, cervical cancer still remains as one of the leading causes of death among women in developing countries. Over 85% of new cases of cervical cancer and deaths due to cervical cancer occur in developing countries where screening programs for early detection are either inadequate or unavailable. While early detection (Papanicolaou smear) and treatment of cervical precancerous lesions effectively prevent the development of invasive cervical cancer, limited resources and infrastructure make it difficult to implement standard cervical cancer screening methods in low-resource areas

One of the primary objectives of Dr. Richards-Kortum Research lab at Rice University is to develop cost-effective optical imaging and spectroscopy tools to reduce the incidence and mortality of cancer and infectious disease through early detection at the point-of-care. The optical imaging tools developed in her lab are based on quantitative imaging methods and integrate advances in nanotechnology, computer algorithms and molecular imaging with microfabrication technologies to provide rapid and robust point-of-care diagnosis, this enables the evaluation of epithelial cell morphology in vivo, in other words it allows to be able to detect cancerous cells in real time without the need of expertise or follow up. This imaging tools are called High Resolution Micro Endoscopes (HRME), unfortunately the cost of these imaging tools are still a barrier to wider scale implementation.

Having these issues in mind I worked on a variation of the HRME called the PI-HRME, a low-cost high resolution micro endoscope. Which still allows for real time imaging of tissue with sub-cellular resolution. The PI-HRME follows the same principles of an HRME but it's attached to a Raspberry PI 2, which is a cheap ($35) programmable single board computer, it also has a touchscreen monitor attached to the case, a 6600 mAH batter, and a user friendly software to be able to read data and capture images. In comparison, the PI-HRME is cheaper than the current computer based HRME, and its able to run imaging software algorithms to automatically detect the presence of abnormal cells, which gets rid of false positives due to human error.

The PI-HRME solves most of the disadvantages of a Pap smear in developing countries; By having a monitor the data is easy to read and with the future implementation of an algorithm to detect abnormal cells expertise wont be necessary at all. Also with the Raspberry Pi 2 being the soul of the HRME the price becomes way more accessible, having a battery included solves the need of electricity to use which is helpful because in some areas where studies are going to be made electricity may not be available, with the small size and weight mobility becomes really easy and because the Pi-HRME does not use any reusable materials it can be used over and over

again without any trouble. Currently the PI-HRME is being used for the detection of cervical cancer, but it can also be modified to work with other type of cancers.
Results suggest that the PI-HRME shows promise to improve cervical cancer screening in resource-constrained settings. The goals of reusability, cost effectiveness, cell imaging portability and no need of external hardware were achieved. The first batch of Pi-HRMEs has already been taken to El Salvador to take part in a cervical cancer clinical study of 3000 patients. If the results are good and pathologists like it, the Pi-HRME might be permanently implemented into developing countries clinical programs.

SECOND PLACE UNDERGRADUATE – ENGINEERING/TECHNOLOGY

Generating Real-Time Musculoskeletal Models Using a Motion Capture System

A. Tamimi and E. Demircan
California State University, Long Beach, Long Beach, CA 90840

Keywords: Musculoskeletal modeling; real-time biofeedback; motion capture; rehabilitation; biomechanics

Musculoskeletal modeling has been widely used to study human movement and to aid in treating and preventing musculoskeletal diseases. The musculoskeletal models are used to estimate internal loading (i.e., knee joint loads) and external measurements (i.e., ground reaction), thus replicating natural human movement. Musculoskeletal models can be combined with human motion capture data to analyze movement and generate subject-specific dynamic simulations. This data can be used to directly measure the skeletal movement and to estimate forces from motion. Currently, there is a lack of integration of musculoskeletal modeling from motion capture data with real-time simulations. This limits potential applications such as motion training and analysis of movement disabilities. Therefore, it is beneficial to develop a system that would generate a real-time musculoskeletal simulation from the observed motion.

In this project, we aim to develop a system using a computational framework (OpenSim) and motion capture (OptiTrack) that analyzes and generates musculoskeletal models in real-time. We will have subjects walk on a treadmill to capture their motion and forces, and will then live-stream that trajectory data into a MATLAB program that will output the generated model using OpenSim. We will also test the system's feasibility by using that model to calculate the knee adduction moment for each subject. We hypothesize that this system will be effective in generating musculoskeletal models in real-time, and will help improve treatments and interventions of musculoskeletal disorders by providing immediate feedback to patients.

The motion and force data will be collected using a 6-camera marker-based motion capture system (OptiTrack) together with a 32-channel electromyography system (ANT Neuro) and a force plate platform. Fifteen healthy subjects will participate in a pilot study to collect the kinematic data. Reflective markers will be placed on the subjects in the following locations: calcaneus, head of second metatarsal, head of the fifth metatarsal, lateral and medial malleoli, lateral and medial femoral epicondyles, lateral mid-shaft shank (2 markers), greater trochanter, lateral mid-shaft femur (2 markers), left and right anterior superior iliac spines, left and right posterior superior iliac spines, left and right acromion, and seventh cervical vertebrae. The Electromyography (EMG) activity will be recorded for the following muscles: biceps femoris longhead, vastus medialis, vastus lateralis, rectus femoris, medial gastrocnemius, lateral gastrocnemius, and tensor fascia latae. Subjects will first warm up by walking on a treadmill at their preferred speed for 2 minutes, and will then walk for two trials at that same speed for 3 minutes each. The marker data will be captured at 120Hz and filtered using a 4^{th} order Butterworth filter with 15Hz cut-off frequency. The knee adduction moment will be calculated from the ground reaction force.

As the subjects' motion is captured, the OptiTrack system will reconstruct that 2D motion data into 3D coordinates for the position and orientation of the movements in real-time. That data will be live-streamed to a MATLAB program as a .trc file by using NatNet SDK, a client/server networking Software Development Kit (SDK) from OptiTrack. After MATLAB reads the inputted motion file, it will be interfaced with OpenSim, an open-source software that models and analyzes human neuromusculoskeletal systems, to create the model corresponding to the recorded motion coordinates. The MATLAB program will calculate the inverse kinematics, inverse dynamics, and forward dynamics to generate a subject-specific lower-extremity simulation (model Gait 2392) in OpenSim. The knee adduction moment will also be calculated using the equation $KAM_y = r_z GRF_x + r_x GRF_z$, where GRF_x represents the mediolateral ground reaction force, GRF_z represents the vertical ground reaction force, r_x represents the mediolateral distance from the ground reaction force center of pressure to the knee joint center, and r_z corresponds to the vertical distance from the ground reaction force center of pressure to the knee joint center. The model will be generated in real-time, as the motion data is being captured from the subject.

We expect this system to generate an instantaneous musculoskeletal model from OpenSim using the OptiTrack motion capture system and a MATLAB interface. The model generated in this project can be used to further evaluate treatments for patients with knee osteoarthritis. We also expect that the real-time kinematic model will simplify the learning of new motor tasks for subjects when used in interventions. This system can be used to help advance the generation of real-time simulations using various models, including upper and full-body models, while reducing the time required to process and analyze the results. The real-time models can not only be used to provide biomechanical feedback for patients and athletes with musculoskeletal disorders, but they can also be used to improve training and treatments in human movement.

THIRD PLACE UNDERGRADUATE – ENGINEERING/TECHNOLOGY

Thermodynamic Analysis of the Frictionless Damping of a Piston

L. Sotelo-Martin and D. S. Corti
Purdue University, West Lafayette, IN 46516

Introduction

This research revisits the time-dependent behavior of two ideal gases contained within a rigid, insulated cylinder and separated by a piston with different values of its thermal conductivity. Even without friction or other dissipative mechanisms acting on it, the piston will eventually come to rest due to the allowed heat transfer between the gases.

Hypothesis

We studied the effects of the gases' initial properties—temperature, pressure, and volume—on the time-dependent behavior of the system. In order to do so, we introduced two models to simulate the gases' behaviors, one developed in the field of macroscopic thermodynamics and the other developed from microscopic thermodynamics.

Methods

Matlab was used to solve the corresponding equations for each model, thereby simulating the frictionless damping of the piston. We also looked at the behavior of other key thermodynamic properties, such as the time dependence of the system's entropy and the path-dependent values of the work done by each gas. As we started analyzing the system, we followed a similar path in order to analyze differing scenarios: stating assumptions and conditions for the scenario, developing differential equations based on equations of motion and laws of thermodynamics, normalizing the differential equations by introducing characteristic times, and generating time-dependent plots for various scenarios.

For the one-chamber macroscopic system, we set the following assumptions for the system: each thermodynamic property is well defined at any point in time, an ideal gas approximation is valid, chamber walls are rigid and piston slides without friction, and the chamber is adiabatic. Using these assumptions and knowledge of thermodynamics, we developed a specific set of equations to describe this system. For this system, we derived a dimensionless characteristic time in order to make the equations easier to solve in Matlab. We then derived a final set of dimensionless differential equations that were solved with the ODE45 function to achieve the desired plots.

Results

For the one-chamber system, it was observed—as anticipated—that the change in the characteristic time ratio is directly proportional to the frequency of the oscillations. One noteworthy scenario from the plots arises from the initially isothermal plots: initially it was suspected that the pressure difference would only cause a slight temperature offset following with a rapid equilibration. The actual behavior is a really quick and large offset that takes longer than anticipated to equilibrate.

We then used the same procedure but for the two-chamber macroscopic system. The behavior in these plots was fairly similar to that with the one-chamber system, one key similarity is the

behavior of the initially isothermal plots. In this case, the offset in temperature difference also caused an indefinite damping in the two temperature functions. As expected, the pressure functions against piston distance were mirror images of one another.

After analyzing the behavior of these systems on a macroscopic level, we decided to look at them on a microscopic level which included between 50 to 150 molecules—this number was limited by the speed of Matlab. Similar to the macroscopic treatment of these systems, we looked at solely the one-chamber scenario. For this system, the evolution of properties such as average potential energy and compressibility factor with differing densities were studied. Isotherms of different reference temperatures and plots for a range of number of molecules were generated and in general, the average pressure versus density plots trended upward as well as the compressibility factor versus density plots. The average potential energy versus density plots trended downward.

Summary

Throughout the entirety of the research in both the macroscopic and microscopic schemes, our results were consistent with previous results found in literature. If investigating further, it would be interesting to investigate the microscopic regime further as well as the initially isothermal cases in the macroscopic models.

FIRST PLACE UNDERGRADUATE – COMPUTER SCIENCE/ENGINEERING

Detection and Protection against Black Hole Attacks on Wired Networks

B. Cerda, E. Martinez-Belmares, and S. Yuan
Houston, TX 770002

Keywords: Black hole attack, Dijkstra's Algorithm, Hamiltonian cycle, Shortest Path, Wired Network

Modern society is becoming increasingly reliant on the Internet for fast, convenient and reliable communications. At the core of the Internet, routers direct and switch packets originated from many sources at extremely high rate, making routers the primary targets of security attacks. Black hole attack is one of the most serious attacks. Under this attack, a compromised router silently drops all incoming user packets, causing permanent data loss to the user. Black hole attacks may be further categorized into “smart” attacks and “dumb” attacks. A “smart” attack is performed by a compromised router that only drops the data packets but responds normally to control packets; a “dumb” attack is performed by a compromised router who drops both data packets and control packets. It is more difficult to detect smart attacks and to identify the compromised router.

In this paper, we propose the Placebo Packet Protocol (PPP) to detect both types of black hole attacks and to identify the compromised routers on a wired network. With this protocol, a working source node sends a fake data packet, i.e., a placebo packet, along a pre-determined route that traverses all routing nodes. The nodes that support PPP sends an acknowledgement packet back to the source node, then forward the placebo packet to the next node on the predetermined route. The placebo packet has the same structure like a regular user data packet but does not contain actual user data; it is only used as a disguise to trick the malicious node in treating the packet as regular data package, and dropping it. Once the package is dropped, the source node no longer receives any acknowledgements, which indicates the existence of a black hole attack. The source then send additional placebo packets to more nodes in order to locate the malicious one(s).

The PPP utilizes two routing algorithms. A Hamiltonian cycle algorithm is used to generate a route that traverse all nodes in the network. This is the predetermined route to send the initial placebo packet by a source node. By using the Hamiltonian cycle, a source node is able to detect a black hole attack with the minimum number of packet exchanges with other nodes, thus shortens the average time of detecting a black hole attack. The other algorithm is a shortest path algorithm such as Dijkstra’s algorithm, which is used to help locating the malicious node(s) after a black hole attack is detected.

Our analysis and computer simulation confirmed that our approach successfully detect all black hole attacks on a network, and are also able to identify the malicious nodes with a success rate of as high as 97.2%, as long as the number of malicious nodes is less than or equal to half the total number of nodes.

Even when the majority of the nodes are compromised, we can still detect all black hole attacks but it becomes difficult to locate all malicious nodes. Simulations also revealed that the network size is an important factor determining the success rate of identifying malicious nodes. When network size is small, a malicious node may disconnect the network and make it impossible for the working nodes in one part of the network to exchange information with the working nodes in other parts of the network. On the other hand, when network size is big, it is less likely that the network becomes disconnected by the malicious nodes, hence the working nodes are able to communicate with each other and locate the malicious ones.

SECOND PLACE UNDERGRADUATE – COMPUTER SCIENCE/ENGINEERING

How Effective are Different ECG Classification Methods Under the Presence of Signal Noise?

E. Ríos López, B. Marlin, and S. Li
University of Massachusetts at Amherst, Amherst, MA 01003

Keywords: ECG, machine learning, pattern prediction, conditional random fields, sparse coding

With advances in technology and the use of mobile, wireless sensors it has become practical to obtain information pertaining to our health, such as the electrocardiogram (ECG) signal. Innovation has facilitated the continuous study of the heart's electrical activity; furthermore, it has promoted new possibilities of bettering technologies that are dedicated to improving and analyzing human health. It is of great importance that applications like these, especially those dedicated to obtaining ECG signals, keep control of noise and hence bring forth clean and accurate data. Today, many machine learning-based algorithms exist and are being designed for the classification of non-stationary signals obtained from mobile sensors. In this work, our approach consists of studying the behavior of ECG signals and making use of a pattern prediction framework called Conditional Random Fields (CRF) for signal classification. The challenge or goal proposed for this research was to test the robustness of our ECG analysis approach in the presence of different levels of noise and compare it to other existing algorithms used for the same purpose. We hypothesized a pattern prediction approach would be a robust alternative for signal classification even in the presence of high levels of noise.

To design our approach, related useful works were applied and combined to maximize signal classification[1]. We started by using a maxima and minima search algorithm to find the candidate peaks and valleys of the electrocardiogram[2]. Next, a sparse coding algorithm was utilized to capture the higher level features in the local neighborhood of the given candidate points in the signal. We wish to learn an over-complete set of basis vectors to represent input vectors; because, with this, we are better able to capture structures and patterns inherent in the input data.

$$\arg min \,||\, x_n - \Sigma_{k=1}^{K} \alpha_k B_k \,||\, _2^2 + \lambda \,\big|\big|\alpha\big|\big|_1$$

Equation 1: Sparse Coding

Once the features have been extracted, we utilized this information in company with a list of the corresponding labels for each candidate peak and construct a dynamic CRF model. The CRF model studies the signal pattern to achieve global learning by finding the dependence between pairs of labels and between labels and its corresponding feature. When the algorithm is "trained", it is prepared to categorize raw, unlabeled signals.[3]

---

[1] The physiological signals used for this research were obtained from an online signal bank website called PhysioNet.

[2] The ECG signal comprises three waves, which are named "P", "QRS", and "T".

[3] In the following equation, *x* belongs to a peak or valley feature and *y* belongs to any of the labels *"P", "Q", "R", "S", "T",* or *"N"*. *"N"* was used to classify points categorized as noise.

$$Pw(y|x) = \frac{\exp(-Ew(y,x))}{Zw(x)}$$

Equation 2: Conditional Random Fields

After building the computational algorithm to label ECG signals accordingly, we proceeded to a testing phase. The algorithm was fed with signals of different noise levels (some were added to the signals and others already inhibited un-stationary behavior). Results showed high robustness to those that had uncommon signals and, as well, to those that were noisy. The outcome obtained showed that the greater the noise, the greater the error in categorization was going to be. In the presence of clean data, the error percent in labeling ranged from 0 to 1%. Now, in the highest presence of noise utilized, the error was up to 35%. It was also noticed that the higher the number of labeled samples for the training phase, the better the accuracy in labeling the peaks and valleys of the signal.

Consecutively, we continued to even more testing by comparing our approach to existing code dedicated to labeling ECG signals. For this, a state-of-the-art ECG classification method called *Wavedet* was used. *Wavedet* consists in detecting the QRS wave, and then using the R-to-R distance to do a local search of the T-wave and the P-wave. This method showed accurate labeling of clean signals; on the other hand, it did not show robustness to noise. As we increased the signal noise, *Wavedet* started to miss the correct labeling in an elevated matter.
Our ECG pipeline based on CRFs showed to out-perform *Wavedet's* local search strategy at all noise levels applied. However, the performance of both methods showed to degrade with increasing noise. Inclusive, it was perceived that the main drawback of a structured prediction approach is having to label the data by-hand first during the "training" phase. Nonetheless, we show that a small number of training samples gives good prediction error. Another conclusion drawn was that having too many or too few sparse basis components affected the algorithm by causing error or over-fitting. Future prospective work could be training the program with data from a specific user and use the trained model to predict labels of unknown data from other users.

THIRD PLACE UNDERGRADUATE – COMPUTER SCIENCE/ENGINEERING

Nanotechnology Video Game for Middle School Students

D. L. Mockford-Polanco and M. Seda
Electrical and Computer Engineering Department, University of Puerto Rico at Mayagüez, Mayagüez, P.R, 00680

Keywords: nanotechnology, gamification, constructivism, outreach, educational game.

Over the years there has been mounting evidence on the positive academic outcomes of playing video games in high school and undergraduate students. A recent study conducted by Posso, found that students who play online games almost every day score 15 points above the average in math and 17 points above the average in science [1] when tested by exams created by the Programme for International Student Assessment (PISA) that focus in math, science, and reading. However, the study failed to find the correlation between a student's ability to translate the problem–solving skills learned by playing games into identifying problems and generating solutions in other context. This raises the question whether or not video games can be an effective educational tool that can be integrated in schools curriculum.

The Nanotechnology Center for Biomedical, Environmental and Sustainability Applications has as one goal, to increase awareness of high school students about nanotechnology and the STEM fields. Nanotechnology is the science, engineering, and technology conducted at nanoscale. Because of our collaboration with the center we are creating a video game themed around the subject of nanotechnology.

The project has been divided in two different phases: (1) storyline and context design and (2) software design. This work presents the storyline and context design part of the Nanito Videogame.

A story that functions as the students' main source of exposure on the nanotechnology subjects was developed with an overall plot, setting, and two playable characters: Nanito (male) and Nanita (female). Nanito and Nanita are fictional characters used to represent the small scale world. The player's interactions with the game were developed according to genre conventions. Level 1 and 3 is a platformer. A platformer is a game where the character can move from left to right and do basic operations such as puzzle solving. The mechanics in these levels are moving left and right on screen, jumping, launching projectiles, and engaging with Non playable character (NPC's). Level 2 is a driving game with the mechanics of accelerating, reversing, and steering left or right. Once the mechanics were established puzzles and problems that test the students' knowledge were created integrating the constructivist learning theory and gamification.

The constructivist learning paradigm, which states that learners construct knowledge for themselves---each learner individually (and socially) constructs meaning---as he or she learns [2], was selected because of its similarities with the ideas in "Gamification", which is the process of using gaming elements in a non-gaming context. These gaming elements can be categorized as mechanics, define the way games (as systems) convert specific inputs into specific outputs,

dynamics, guide how players and the game mechanics interact during the game, and aesthetics, which refer to the way the game mechanics and dynamics interact with the game designer's artistry, to produce cultural and emotional outcomes [3].
We hypothesize that students who learn about nanotechnology using the Nanito video game will be more engaged and interested in the subjects of nanotechnology and STEM fields, and score higher in the tested subjects, when compared with students who did not.

The ideation process consisted of each member of the GameDev group reading about the fundamental concept in nanotechnology, summarizing, and brainstorming different ways to adapt in the story, game mechanics, dynamics, and aesthetics the concepts and discoveries from nanotechnology that could interest students. The subjects chosen were ferrofluids, the improvements of photovoltaic solar electricity generation with nanotechnology (solar power) [4], and nano-textiles. The designs were collected and streamlined and discussed with the programming team to include feasibility in the decisions. Programmers the proceeded with coding and instantiation. Designs were modified based on the final implementation details.

We are currently in the programming phase of three different levels. We will use a qualitative research method to describe student engagement. These will be conducted in schools using a group of students that will learn by playing the game and another group that will be taught through traditional methods. Qualitative data will be collected using face to face interviews and focus groups of 6 to 8 people. They will be observed and asked about their experience with the game and what they have learned.

We predict that students that play the Nanito video game, will be more engaged and show more interest in Nanotechnology than those who do not.

In conclusion, with the completion of the first 3 levels (ferrofluids, solar power, and nano-textiles) of the game, we can begin testing the game at the middle school level to determine how effective gamification is as a learning tool.

References:
[1] Posso, A. (2016). Internet Usage and Educational Outcomes Among 15-Year Old Australian Students. *International Journal of Communication*, *10*, 26.
[2] Bhattacharjee, J. (2015, July). Constructivist Approach to Learning– An Effective Approach of Teaching Learning [Abstract]. *International Research Journal of Interdisciplinary &, I*(VI), 65-74.
[3] Dicheva, D., Dichev, C., Agre, G., & Angelova, G. (2015). Gamification in education: a systematic mapping study. *Educational Technology & Society*,*18*(3), 1-14.
[4] NSI: Nanotechnology for Solar Energy Collection and Conversion-- Contributing to Energy Solutions for the Future. (n.d.). Retrieved August 11, 2016, from http://www.nano.gov/NSISolar

FIRST PLACE GRADUATE – MATH/SCIENCE

Predicting Diabetes: A Predictive Analysis of Human Pancreatic Cell Types

M. Santana and E. Yang
University of Houston-Downtown, Houston, TX 77002

Keywords: diabetes, bioinformatics, predictive analysis, pancreatic islet, predictive genomics

As of 2012, diabetes is the seventh leading cause of death in the United States. It is estimated that approximately 29 million Americans have diabetes, with 8 million cases being undiagnosed. 1.4 million new cases are diagnosed each year. Doctors are aware of certain characteristic factors which mark patients as having a predisposition for diabetes, such as dietary and environmental factors, family history, and even geographical location. However, efforts to expand knowledge in regards to a more genetic basis of diabetes is underway, especially through the use of predictive analytics. This project seeks to perform a predictive analysis on the single-cell RNA sequencing of pancreatic islet cells. Among the cell types contained within is insulin (beta cell), damage to which is known to be a cause of diabetes. It is our aim to be able to accurately predict the occurrence of diabetes based purely on an analysis of the patients' genetic data.

Our hypothesis in this project is primarily in regards to the approach of the analysis. It is our belief that, rather than identifying individual genes that are conducive to the prediction of diabetes, that prediction will be much more effective when performed on clusters of genes. It is our aim, therefore, to cluster genes into various compositions of sub-types based on relative similarity with regard to endocrine cell type. Furthermore, we are specifically seeking clusters of gene expressions that are most effective at predicting both the pancreatic cell type and the likelihood of diabetes in a patient.

The dataset used for this analysis is contained within the Gene Expression Omnibus (GEO) database and is relatively recent, being published in August 2016. In the data there are 1600 samples of the expression of nearly 40,000 genes from human pancreatic islets. There are two response variables around which the analysis is being conducted, one regarding the condition of the cell (diabetic or non-diabetic) and another regarding the cell's subtype (alpha, beta, delta, epsilon, and PP). The problem will be approached in two ways. One is to consider cell type as the singular response; the other is to be able to both predict the cell type and the occurrence of diabetes, together. Therefore, two separate but related analyses will be performed.

The overall process of the analysis takes three general steps. Due to the significant number of unexpressed genes present in the dataset, a great deal of feature selection and dimension reduction is necessary. Therefore the first goal is to limit the number of genes to those most primarily influencing the overall model. Methods such as principal component analysis are used here, but not exclusively. The second step is to then attempt to cluster the genes. Methods used in this regard are various implementations of k-medoid, class prototyping, non-negative matrix factorization (NMF), hierarchical ordered partitioning and collapsing hybrid (HOPACH), as well as others. The goal is to seek the minimum amount of clusters while still maximizing their predictive quality. The third and final step is to perform prediction based on these

clusters. Throughout the process, k-fold cross validation will be used to judge the performance of the models. The metrics used to evaluate model performance will be an accuracy score and a logloss function.

Currently, analysis is still being completed. Preliminarily, the use of t-distributed stochastic neighbor embedding (t-SNE) was very helpful in the demonstration of proper separability of the data, indicating its conduciveness to clustering. The clustering methods that are most effective primarily involve the use of medoids. Class prototyping produces the most efficient clustering, where a prototype of a cell type is created by organizing samples by cell type and then using the mediod of that cluster as a representative of the class for prediction. However, more accuracy comes from k-mediod methods allowing for more clusters, rather than simply sorting solely by type. It is for this reason that more testing to define the best number of clusters is being further investigated. Through cross validation, results seem to indicate that the methods generalize well.

Doctors and researchers have been aware for some time about the genetic predisposition that underlies the occurrence of diabetes. With the development of effective methods for genetic sequencing, that predisposition now lends itself to full predictive analysis. However, with the vast number of genes to predict from, it is most likely a clustered subset of genes that provide the greatest predictive power. Identifying these clusters would greatly aid not only our understanding of the ways in which pancreatic cell types contribute to diabetes, but also aid doctors in providing preemptive and anticipatory measures for patients with a greater likelihood of diabetes at a very early stage.

SECOND PLACE GRADUATE – MATH/SCIENCE

The Use of Microfluidic Device "Labyrinth" for Early Detection of Pancreatic Cancer

L. Rivera-Báez[1], E. Lin[1], M. Lee[1], M. Waghray[2], H. Cameron[2], E. Azizi[3], S. Fouladdel[3], V. Sahai[3,4], M. Wicha[3,4], D. Simeone[2,4], and S. Nagrath[1,4]
[1]Department of Chemical Engineering, University of Michigan, Ann Arbor, MI
[2]Department of Surgery, University of Michigan, Ann Arbor, MI
[3]Department of Internal Medicine, University of Michigan, Ann Arbor, MI
[4]Translational Oncology Program, University of Michigan, Ann Arbor, MI

Introduction

Pancreatic cancer is a devastating disease with the highest mortality rate among all cancer types. Therefore, it is imperative to search for informative and specific biomarkers for metastatic pancreatic cancer that would lead to early diagnosis. Emerging evidence has pointed the importance of circulating tumor cells (CTCs) in the spread of cancers and metastasis. CTCs are believed to be the most promising cancer biomarkers available in blood that could be used for not only prognosis, but also for cancer detection and development of personalized treatment. Here we present a complete label free technology to isolate CTCs from whole blood at a high throughput of 2.5mL/min in a single step. Using the Labyrinth we aim for the isolation of different CTC subpopulations in cancer patients. Once CTCs are isolated, a comprehensive functional characterization would provide an insight into their biological relevance.

Materials and Methods

Labyrinth Fabrication. The mold for the polydimethylsiloxane (PDMS) device is formed from a negative photoresist SU-8 100 patterned using standard soft lithography techniques.

Labyrinth Optimization using cell lines. Device is pre-flowed with 1% Pluronic acid solution (diluted in 1X PBS) at 100 µL/min for 10 minutes to prevent cell clotting on channel walls. Labyrinth is filled with buffer sample at different flow rates and is observed under microscope. Waste from each outlet of Labyrinth is collected for cell counting to calculate the recovery percentage.

Patient Sample Processing. Labyrinth is pre-flowed with 1% Pluronic acid solution (diluted in 1X PBS) at 100 µL/min for 10 minutes to prevent cell clotting on channel walls. Blood sample is then processed through the device, at a flow rate of 2.5 mL/min. Flow stabilization takes 1 minute, so recollection of the second outlet starts after 1 minute.

Results and Discussion

Labyrinth was optimized for pancreatic cancer samples, where optimal cell purification was obtained at 2.5 mL/min, having 92% of PANC-1 recovery from the second outlet and with a high white blood cells (WBC) removal of 89% into the first outlet. In addition, cell viability was assessed using the MTT assay to ensure potential of downstream analysis. Cells processed in

Labyrinth started proliferating just 24 hours after being incubated, increasing their population by 50% within just three days. This preliminary result demonstrates that the shear stress that cells experience in Labyrinth does not have a significant effect on their viability or their proliferation rates. Over 100 clinical samples have been processed through the Labyrinth, resulting in an average of 28±24 CTCs/mL across pancreatic cancer patients. Additionally, some samples were characterized using different markers that range from epithelial (CK) to mesenchymal-like (ZEB1) phenotypes, showing the vast heterogeneity among CTCs.

Figure 1. Optimization of Labyrinth.
a) Flow rate optimization of Panc1 cell lines. b) Recovery of WBCs and CTCs from Labyrinth.

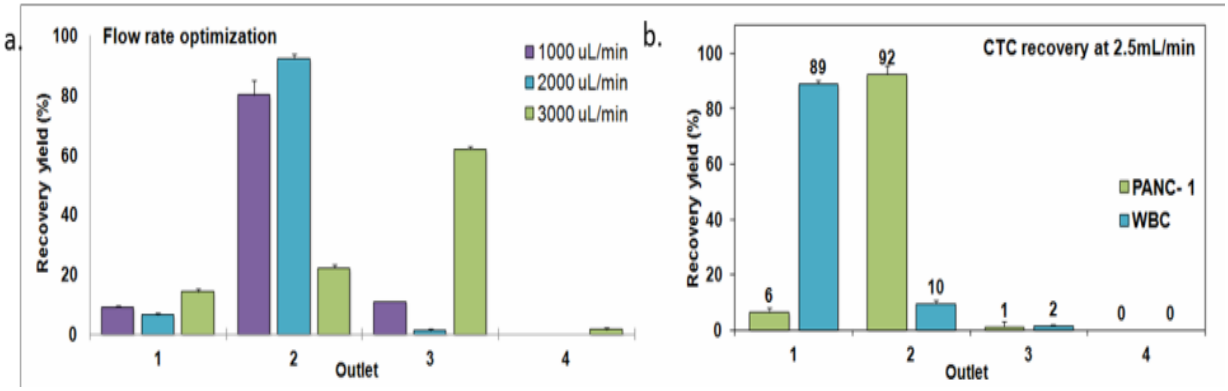

Conclusions

To improve treatment outcomes for pancreatic cancer patients, a broader understanding of the biology of metastasis is necessary. The Labyrinth enables a high throughput separation of several subpopulations of CTCs in a label free matter. The characterization followed by the Labyrinth allows the comprehensive study of patient- derived CTCs; in order to elucidate the most aggressive subpopulations within CTCs for its use as a prognostic tool. The isolation and characterization of CTCs, the heterogeneous population of cells that promote metastasis, can provide meaningful information to elucidate the process of pancreatic tumorigenesis to preempt its fatal result.

THIRD PLACE GRADUATE – MATH/SCIENCE

The Effect of Three Exogenous Biostimulants in Fruit Yield and Attributes when Applied During Fruit Development of the Pulasan (*Nephelium ramboutan-ake*)

Z. Rodríguez-Pagán[1], J. P. Morales-Payán[1], R. Goenaga[2] and A. Segarra[1]
[1]Departament of Agro-Environmental Sciences, University of Puerto Rico at Mayagüez
[2]Tropical Agriculture Research Service (TARS), University of Puerto Rico at Mayagüez

Keywords: Pulasan, *Nephelium ramboutan-ake*, exotic fruit, biostimulants, fruit yield

The market for exotic tropical fruits imported to developed countries has been increasing in the last 20 years. Fruits belonging to the Sapindaceae family, among them the pulasan (*Nephelium ramboutan-ake*), are receiving special attention in that market. The pulasan represents an alternative for growers in Puerto Rico who are searching substitutes for coffee (*Coffea arabica*) and citrus (*Citrus* sp.) orchards, considering that both crops have been recently affected by new pests (*Hypothenemus hampei*) and diseases (Citrus greening) that may greatly decrease yields. The pulasan is also an option for growers searching for high-profit fruit crops, as the price of fresh pulasan fruits fluctuate between $4 and $7 per pound in Puerto Rico and the United States mainland, respectively. At the same time, organic exotic fruits are considered a niche within a niche. Organic pulasan may reach even higher prices, which is the reason research aimed at increasing fruit number, size, and/or quality of the pulasan using organic bioestimulants would be welcome by growers. Biostimulants are commercial inputs based on organic exogenous substances, of natural or artificial origin, which in relatively low concentration have similar effect to those of phytohormones. Biostimulants have been used to increase yield and/or quality in several fruit crops, but there is no documented research on their effects on the pulasan.

We hypothesized that biostimulants applied to trees during the fruit development stage may have a positive effect on fruit yield and quality attributes, which would result in benefits for growers.

Research was conducted in 2014 in a commercial orchard of pulasan in Mayagüez, Puerto Rico, to assess the effects of three bioestimulants on pulasan fruit yield and attributes. A completely randomized design with 8 trees per treatment was used. Treatments were foliar sprays of a water-diluted commercially-available formulations of (a) free amino acids fortified with potassium (MAA) applied at 7.4 ml/tree every 14 days, (b) an extract of the marine algae *Ascophyllum nodosum* (AN) at 7.4 ml/tree every 14 days, and (c) an extract of Caryophyllaceae and Fabaceae plants (ECF) at 370 mg/tree every 28 days, as recommended by manufacturers. Bioestimulants were first applied when fruits were on average 27 mm in diameter. A check group without biostimulants application was used for comparison. The trees were managed organically, except for trees treated with the amino acid mix, which is not certified as an organic biostimulants.

Even were no difference in fruit yield was found when compare biostimulants treatments with the control group (125.93 kg) when compare biostimulants treatment between them, MAA were higher (254.74 kg) in contrast to AN (179.84 kg). The percent of commercial fruit was 86%, 80%, 75% and 67% for AN, ECF, MAA and control group respectively. Fruits from trees sprayed with biostimulants had higher fruit diameter than control group (50.15 mm), with 55.26 mm, 55.12 mm and 54.12 mm for AN, MAA and ECF and also the fruit length was higher in AN

treatment (64.54 mm) when compare with the control group (59.50 mm). Intact fruit weight, pericarp and aril weight were positive affected by bioestimulants when compare with the control group.

The results show that fruit yield (fruit weight per tree) of biostimulants-treated trees was not significantly enhanced as compared to control trees, which does not benefit growers selling the fruit by weight. However, biostimulants that reduced fruit number per tree resulted in increased individual fruit size and weight, which may be economically advantageous for markets paying higher prices for larger fruits. This research demonstrates that pulasan fruit size and weight may be manipulated with biostimulants. Future research will study the effects of timing, rate, and mode of application of these and other biostimulants searching for treatments to improve pulasan fruit number and individual fruit weight.

Acknowledgment: The authors thank the owner and crew of Panoramic Fruit Farm (experimental site), and advise from Professor José Zamora and Dr. Lydia Rivera from the UPR

FIRST PLACE GRADUATE – ENGINEERING/TECHNOLOGY

Yttria Rich TBCs as Candidates for CMAS Resistant Top Coats

J. J. Gomez Chavez[1,2], R. Naraparaju[1], U. Schulz[1], and C.V. Ramana[2]
[1]German Aerospace Center (DLR), Institute of Materials Research, Cologne 51170, Germany.
[2]Department of Mechanical Engineering, University of Texas at El Paso, El Paso, TX 79968

Keywords: TBC, reaction products, EB-PVD, glass infiltration, CMAS.

State of the art thermal barrier coatings (TBC) commonly made of 7-8 wt. % Yttria Stabilized Zirconia (7YSZ) are used in modern gas turbines to generate thermal protection to the underlying super alloy components enabling engines to operate at higher temperatures than the super alloy melting point (>1200°C). TBCs allow higher operating temperatures for hot gas path components, thus, generating higher engine efficiency. The common TBC production methods are air plasma spray (APS) and electron beam physical vapor deposition (EB-PVD) which generate a porous microstructure with a low thermal conductivity. The current demand for more efficient gas turbine engines is pushing for operating temperatures up to 1300°C at which standard 7YSZ materials phase significant limitations such as phase transformation and hot corrosion which reduce engine lifetime and performance. The infiltration of molten glassy mineral deposits composed of CaO-MgO-Al_2O_3-SiO_2 (CMAS) represents one of the major threats in reducing performance and service life in aero and land based gas turbine engines. The CMAS deposits are ingested into the engine carried commonly in sand, runways debris, fly ash and volcanic ash. The ingested particles melt on the engine's hot gas path components infiltrating the porous TBC, this infiltration generates detrimental effects on the coating such as microstructural degradation and strain tolerance reduction.

This research proposes a CMAS protective overlay coating based on a sacrificial oxide layer that vigorously reacts with the CMAS compounds inducing their crystallization, thus, avoiding further infiltration. The proposed coating can be deposited on top of a standard 7YSZ coating generating a multilayer TBC system. Thus, the multilayer TBC can be composed of the top sacrificial CMAS protective oxide layer and the undelaying layer of standard 7YSZ for thermal insulation.

The present work studied in detail the resistance of CMAS infiltration in yttria rich-zirconia based coatings (150 µm thick) by testing a protective EB-PVD –top-coating with higher amounts of yttria (Y_2O_3). Studies were made with Y_2O_3 rich top-coatings with an yttria content ranging in 65 wt. % (rest is zirconia). Samples were deposited using a jumping beam system with dual evaporation sources composed of standard 7YSZ and pure Y_2O_3. The evaporation technique did not allow high control of the evaporation rate generating higher porous columnar structure compared to standard 7YSZ generated microstructures. CMAS infiltration experiments were performed at 1250 ºC -at time intervals from 1 to 20 hours for long term infiltration and 5 minutes for rapid infiltration using two real volcanic ashes and a model CMAS source for results comparison. The infiltration experiments were performed by depositing CMAS on top the coatings in the amount of 20 mg/cm^2 and heat treated as specified above. The volcanic ashes were collected from site from the Eyjafjallajökull volcano located in Iceland and the Sakurajima

volcano located in southern Japan. The synthetized CMAS composition was generated by matching the chemical composition obtained from studies performed on real engines under CMAS attack.

The results showed a high CMAS resistance by inducing crystallization of the CMAS glass due to a formation of stable oxyapatite and new garnet phases which have not been previously reported. The formed crystalline phases conglomerated at the coating/glass interphase forming a stable reaction layer which effectively blocked the porosity features of the coatings avoiding further CMAS glass infiltration. The morphology of the reaction layers varied for the volcanic ashes and synthetized CMAS which proves a different reaction nature for natural CMAS sources compared with synthetized sources. Additionally, the CMAS arrest reaction layer exhibited a minimal growth (<30 µm after 20 h) making yttria rich-zirconia coatings promising candidates for CMAS resistant multilayer TBCs. The results also proved a dependency of coating microstructure for infiltration resistance suggesting that the infiltration resistance can be further improved by refining the TBC microstructure by maintaining a densified morphology.

CMAS resistant top coats were produced by EB-PVD system based on yttria rich-zirconia with a nominal 65 wt. % Y_2O_3 and rest ZrO_2. The coating exhibited promising results for CMAS infiltration resistance by generating stable reaction products that crystallized the glass preventing from further infiltration.

SECOND PLACE GRADUATE – ENGINEERING/TECHNOLOGY

PTEN Deletion in Pancreatic Cancer Associated Fibroblasts Decreases Hydraulic Permeability Independent of Collagen Fiber Alignment in a 3D Microfluidic Model of the Tumor Stroma

A. Avendano[1], J. Chang[1], C. Ennis[2], A. Stratton[3], J. R. Pitarresi[1], M. C. Ostrowski[1], and J. W. Song[1]

[1]The Ohio State University, Columbus, OH 43210

[2]Kenyon College, Gambier, OH 43022

[3]Lehigh University, Bethlehem, PA 18015

Keywords: Pancreatic cancer, cancer associated fibroblasts, microfluidics, hydraulic permeability, collagen fiber alignment

Pancreatic ductal adenocarcinoma (PDAC) is one of the deadliest malignant solid tumors, with an overall 5 year survival of 5% and no established effective therapies. PDAC is unique when compared to other tumors in that the majority of cells composing the tumor are not cancer cells but other cell types such as fibroblasts, immune cells, and endothelial cells that exist in areas surrounding the tumor (known as the tumor stroma). The tumor stroma has emerged as an important mediator of pancreatic cancer growth and metastasis to distant sites of the body. In particular, loss of the tumor suppressor gene phosphatase and tensin homolog (PTEN) in pancreatic cancer associated fibroblasts (CAFs) within the tumor stroma has been shown to accelerate tumor progression and therapeutic resistance, resulting in a more aggressive form of PDAC. However, knowledge of how loss of PTEN in CAFs function to produce this effect is limited, due in part to difficulties of current *in vitro* approaches to model the tumor stroma and *in vivo* approaches to isolate and quantify the individual effects of CAFs.

Using a microfluidic 3D model of the tumor stroma, this study set out to characterize how loss of PTEN in CAFs enable these cells to alter two biophysical properties of the tumor microenvironment: i) collagen fiber alignment and ii) hydraulic permeability or the ability of fluid to flow through a porous medium. Aligned collagen fibers have been shown to provide contact guidance for tumor cells to metastasize while hydraulic permeability is an indicator of how well flow and drugs can penetrate into the tumor and thus provide important parameters to profile the effects of CAFs in PDAC. We hypothesized that loss of PTEN would result in more aligned collagen fibers and decreased hydraulic permeability, characteristic of very aggressive PDAC.

To evaluate our hypothesis, a microfluidic model of the tumor stroma was designed, fabricated, and optimized to measure collagen fiber alignment and hydraulic permeability as a function of PTEN deletion in CAFs. The microfluidic model consisted of Polydimethylsiloxane (PDMS) devices fabricated using traditional soft lithography methods. The devices consisted of a single straight channel (5 mm long, 500 um wide, and 1mm tall) with 4mm inlet and outlet ports. Pancreatic CAFs, isolated from human pancreatic tumors, were then suspended in a rat tail type I collagen hydrogel, injected into the channel, and cultured between 1-2 days for hydraulic permeability measurements or 4 days for collagen fiber alignment measurements. The

conditions tested were control pancreatic CAFs (shnc), pancreatic CAFs with PTEN silenced with shRNA (shPTEN), and acellular collagen Type I hydrogel.

The hydraulic permeability was determined by flowing a rhodamine-bovine serum albumin dye through the channel and measuring the average fluid velocity through the collagen type I hydrogel. Darcy's Law for flow through porous medium was then used to calculate the hydraulic permeability. Collagen fiber alignment was assessed by taking confocal reflectance images of the collagen fibers within the device and post processing with an in house made Fast Fourier Transform Matlab algorithm. The algorithm calculated an alignment index, a ratio between the frequency of the most aligned region of the image and the ideally random case. With this criteria, alignment indices closer to 1 indicate random alignment while higher values indicate more aligned collagen fibers.

We detected no significant differences in collagen fiber alignment when comparing shnc, shPTEN, and acellular collagen conditions. In contrast, the hydraulic permeability decreased significantly for the shPTEN condition ($p<0.005$) when compared to both shnc and acellular collagen conditions. These results indicate that loss of PTEN in CAFs results in decreased hydraulic permeability of the tumor stroma that is independent of collagen fiber alignment. Furthermore, the decrease in the hydraulic permeability conferred by shPTEN fibroblasts can explain why loss of PTEN in pancreatic tumors results in resistance to therapy since decreased hydraulic permeability impedes delivery of therapeutic agents into the tumor. Since fiber alignment was not observed to be impacted by expression of PTEN in CAFs, we suspect that this decrease in hydraulic permeability is mediated by the deposition of extra-fibrillar matrix molecules that increase the hydraulic resistance through the porous medium.

Future studies will use our developed *in vitro* system to investigate what biochemical changes occur in the stroma as a function of loss of PTEN in CAFs, and to develop strategies to prevent/reverse this effect. This approach can potentially yield new therapeutic strategies to contain PDAC and improve the poor outcome of current standard of care therapies for pancreatic cancer.

THIRD PLACE GRADUATE – ENGINEERING/TECHNOLOGY

Characterization of Deposits Formed on *Columbia* Space Shuttle Carrier Panel Tiles and Thermal Pane Glass Debris

B. Arellano, M.J. Contreras, S.W. Stafford, D. Cone, and J.D. Olivas
The University of Texas at El Paso, El Paso, TX 79968

Keywords: re-entry effects, thermal protection system, thermal pane glass, deposit formation, characterization

Crew safety has been the focus in developing future manned spacecrafts such as NASA's Orion program. Events in the past, although tragic, have provided the opportunity to incorporate safety lessons learned from the disaster that took place on February 1, 2003. A piece of insulating foam from the external tank impacted the edge of the left wing after launch causing failure of the orbiter and loss of the seven crew while returning to earth's atmosphere. Because the orbiter experienced extreme temperatures, hypersonic velocities, and break-up; further examining these effects on orbital materials can provide insights onto how they react under such conditions.

The aim of this research is to examine the material behavior of the debris to provide the aerospace community with additional evidence onto how these materials react under harsh environments. The debris contain unique characteristics that have yet to be thoroughly examined thus, the thermal protection system (TPS) located on window 7 will be the focus of research along with the protective outer glass thermal pane. These two material systems played a major role in the operation of the orbiter because they experienced extreme temperatures and protected the underlying structural materials. This is important because new developments in commercial space flight or future manned space flights, will require the use of TPS. These materials must be continued to be studied aggressively to provide risk assessment for future missions.

Studies on microstructural investigations after plasma re-entry exposure have been limited on shuttle TPS. However, char deposits were initially found on overhead window 8 windshields. The "char layer" was made up of a primary layer of TiO_2 crystals, a second layer mixture of TiO_2 and Al_2O_3-SiO_2-TiO_2, followed by an aluminum deposition. This investigation will determine the existence of layered metallic deposits and degradation behavior on recovered carrier panel tiles. Another characteristic to be determined is the source of metallic deposits which may have originated from a component directly near the orbiter windows. Two payload bay latch rollers comprised of a Ti-6Al-4V alloy contained evidence of heavy erosion that may have contributed to the source of titanium. Deposits of molten aluminum may be expected as the shuttle framing is composed of an aluminum alloy. Exploring the behavior of titanium under extreme environments is necessary as titanium alloys are a common aerospace material that may have combustion characteristics.

The methods and procedures for analyzing these materials include non-destructive and destructive evaluations. Non-destructive evaluations involved visual inspection, 3D modeling, and surface x-ray fluorescence (XRF) analysis. Visual examination was necessary to locate areas of interest and macroscopic surface flaws. 3D modeling was used to provide additional documenting of the as-received conditions. The elemental composition of the material surfaces

was obtained by utilizing a handheld XRF analyzer. En route to metallography, samples were sectioned by using a rotary cutting tool and fine jeweler's saws. Metallography was performed for examining cross-sections for deposits that included sectioning, mounting specimens in epoxy mounts, grinding, polishing, and cleaning. Tile and glass fragments were characterized by analyzing microstructural features through scanning electron microscopy (SEM) and acquisition of energy dispersive spectroscopy (EDS) spectras. Finally, x-ray diffraction (XRD) will be carried out to confirm the identity of surface deposits.

Upon visual examination of the tiles, areas of thermal alterations were observed in forms of slumping of the TPS coating, exposed tile fracture surfaces, small indentations, and discolorations on surfaces. The remaining thermal pane glass contained fracture surfaces and a dark opaque coating. Surface XRF results have shown three major elements of aluminum, titanium and silicon. The weight percentage of titanium seemed to increase when analyzing the colored deposits. XRF results of the glass fragments detected a variety of major and trace elements such as aluminum, silicon, titanium, iron, and copper. Cross-sections of TPS samples analyzed by SEM demonstrated heavy porosity and severe cavities present throughout the coating. Elemental EDS spot and area measurements revealed titanium oxide (TiO), aluminum, calcium, and silicon characteristic peaks present only on TPS coating. EDS results obtained from a glass fragment cross-section also detected similar major elements. XRD elemental surface analysis is anticipated to measure comparable EDS results.

The alterations experienced by the debris were studied by conducting materials characterization to investigate metallic depositions, plasma flow characteristics, and overall degradation. The plasma flow emanating from the re-entry environment may have affected the surface of the tiles causing depositions and slumping to occur on the TPS coating. Tile and glass surfaces and cross-sections contained titanium, silicon, and aluminum. Therefore, a titanium source must have been present near the orbiter window. The "char layer" that was previously examined, also exists in the TPS coating of the tiles. Thus the elemental and compound analysis will ultimately permit us to gain knowledge of these aerospace materials reactivity to re-entry environment to avert future disasters.

FIRST PLACE GRADUATE – COMPUTER SCIENCE/ENGINEERING

Integrating ARM Devices Into Cloud Infrastructure

P. Kumar and E. Arzuaga
University of Puerto Rico, Mayagüez, Puerto Rico 00680

Keywords: virtualization, heterogeneous cloud computing, ARM-based embedded cloud, KVM on ARM.

Regardless of the type of user, be it a computer professional or smartphone user, working in a small bank or at a high tech IT company, everyone is knowingly or not using cloud-computing. In fact, the cloud-computing model provides various advantages over traditional computing in terms of service availability, scalability, processing and administration. Further, the cloud-computing framework relies on the principle of sharing resources and underlying hardware architectures through the virtualization of various components through software interfaces.

Increasing popularity of ARM-based boards with multi-core processors, along with commodity hardware components with cost-effective power consumption, yet smaller and compact design, has exposed a wide range of opportunities to positively impact computing infrastructure such as redefining building blocks for parallel computing, virtual computing, cloud computing, high performance computing, and real-time computing. With widespread availability of such hardware, nearly anyone can now build a specialized hardware solution to meet required application's performance, cost or power consumption.

This work is undertaken to study and evaluate the use of virtualization to build a cloud system on ARM-based embedded boards. In particular, this work will focus on the understanding of how effectively virtualization works on embedded boards and how this idea could be further nurtured to develop a whole cloud based service that provides virtual machines (VMs) on demand. We will discuss various techniques for setting up VMs using open source and publicly available software and tools on ARM-based boards. Our goal is to provide a system that is able to run common desktop operating systems in currently standard architectures, such as Windows and Ubuntu on x86 as well as the capability of supporting native ARM-based operating systems with full KVM/QEMU support.

We will use ARM-based ODROID boards which comes with an octa-core processor and 2 gigabyte of RAM. For example the ODROID-XU4 has a hardware configuration of a 2 Quad-core CPU (Cortex A15 with KVM extensions & Cortex A7), 1 Gigabit Ethernet, 2 gigabyte of low power RAM and all the peripherals required to convert it to a minicomputer running Linux/Ubuntu(14.04 LTS). We have made preliminary performance tests by running Dhrystone and Whetstone benchmarks on these boards. Further, these benchmarks have provided us with a vision as what we can expect in terms of running virtualized solutions on these small boards. We further divided our work based on the placement of benchmark under different scenarios. Such as running:

- Benchmarks natively and pinned to one Cortex-A15 core.
- Benchmarks natively and pinned to one Cortex-A7 core.

- Benchmarks in a Ubuntu-armhf VM running on top of host OS using one CPU with KVM.
- Benchmarks in a Ubuntu-armhf VM running on top of host OS using one CPU but without KVM extensions.
- Benchmarks in a Ubuntu-x86 VM running on top of host OS using one CPU.

As Dhrystone small size allows it to easily fit inside processor caches but after adding few thousand loops the score remains constant and scales linearly for clock speed. We collected Dhrystone and Whetstone output by running it multiple time and progressively increasing the number of loops and loop count respectively. The performance results collected are as follow-

Dhrystone MIPS & Whetstone MFLOPS for benchmark running on:

- Native hardware and process pinned to Cortex-A15 core yield ~2334 MIPS & ~680 MFLOPS.
- Native hardware and process pinned to Cortex-A7 core yield ~1040 MIPS & ~375 MFLOPS.
- Virtual Machine (Ubuntu-armhf) using KVM yield ~2221 MIPS & ~655 MFLOPS.
- Virtual Machine (Ubuntu-armhf) without KVM extensions yield ~115 MIPS & ~26 MFLOPS.
- Virtual Machine (Ubuntu-x86) using 1 CPU yield ~420 MIPS & ~96 MFLOPS.

These data suggests that the near native performance can be achieved in virtualized environment on such a specialized embedded hardware using KVM whereas standard x86 operating systems can also take advantage of performance to power trade-off and performance to cost trade-off. Further, the data provides a strong ground to use these boards as a foundation for building more complex ARM based virtual infrastructure for small to medium institutions. Our next goal is to run and compare the query processing benchmarks such as TPC-C and TPC-H on this hardware natively and on supported virtual machines for ARM and x86 architectures. We are expecting our ODROID-XU4 performance under TPC-C and TPC-H to be following similar fashion to what we have seen in Dhrystone and Whetstone benchmark. With TPC-C and TPC-H results we would be able to conclude performance of ODROID-XU4 under real time transactional and analytical systems.

Combining virtualization with this commodity hardware, such as ODROID XU4 systems, we have an excellent platform to build a prototype of our proposed low-powered heterogeneous cloud solutions for commercial, as well as personal requirements to build a cluster and serve as a cloud infrastructure to deploy application servers or on-demand virtual machines.

SECOND PLACE GRADUATE – COMPUTER SCIENCE/ENGINEERING

Ontology-Based Data Integration for Freight Performance Analysis

D. Mejia, M. Chowdhury, J. Caballero, E. Camacho, and E. Torres
The University of Texas at El Paso, El Paso, TX 79968

Keywords: Ontology, Freight Performance, Data Integration, Competency Questions, TripleStore

Throughout the United States freight trucks move products from one place to another using the local roads and interstate highways. At a more specific level the transportation of such freight trucks through a city has a great effect on the roadways and traffic of the city; whether they are involved in traffic jams or accidents. The way a freight truck passes through a city can be analyzed by collecting data from various local, state, or national agencies to help determine the performance and efficiency of moving products within a city.

We hypothesized that we would be able to take multiple data sets of different formats and link them together using ontologies. Furthermore, we also hypothesized that we would be able understand and analyze data of the transportation of freight trucks within a city by integrating it together in an ontology so that an expert in the field could answer relevant competency questions.

Our solution was developed based on the specifications of a Civil Engineer, an expert in freight performance. After providing a set of requirements, foundational understanding of freight performance concepts and data sources we developed an ontology. Ontologies provide an organized approach to integrate unstructured data through objects and relationships. It integrated data from multiple sources and formats to add increased analysis of the domain.

The ontology began with a concept map and analysis of its properties. The concept map organized the sub-domains and organize relationships between different properties. The data sources were parsed from several different formats into a common format. The ontology was created using the OWL API in Java. Each object was explicitly programmed and populated by the data to create the ontology. With the use of generic reasoners, we were able to infer additional information and relationships required to answer competency questions. The completed ontology was then transferred into a *TripleStore* – a database to retrieve semantic queries. Semantic queries provide an efficient way to query the entire ontology since it retrieves only the necessary data based on the meaning of the query. Based on the competency questions that were given by our expert, we created a set of queries to run on the ontology. We used a web-based interface for users to easily run queries and return results.

Our resulting ontology in the *TripleStore* confirmed our first hypothesis; that multiple data sets of different formats would be able to be linked together using ontologies. The second hypothesis was also confirmed and showed the accuracy and completeness of our ontology. Our expert was also able to answer all of the competency questions by running each query made on the ontology. Our results also caused new questions to be developed and new analysis to be made on the data; additional questions being raised help prompt new ideas and research questions.

Our work provided efficient and accurate representation of freight performance in El Paso County (Texas) through the integration of data into a domain specific ontology. Our framework for this work is generic and can be used to integrate data on a larger scale such as a state or country. The results make it clear that this work can be easily transformed to integrate data across multiple domains to increase the efficiency and productivity of analyzing and understanding domain specific data. Domains do not have to be related directly to engineering or other sciences; it has its place in liberal arts research or any field that has data of any sort. The ability to access data in different formats, organize it and query it in a way that humans can understand opens up a platform of new work. Not only can it be used in academic interdisciplinary research, it allows for practical uses in everyday data driven systems.

THIRD PLACE GRADUATE – COMPUTER SCIENCE/ENGINEERING

A Modular Design Approach to Outcome-Based Embedded System Design Education

D. Rojas, M. Jiménez, and A. Santiago-Román
University of Puerto Rico at Mayagüez, Mayagüez, PR 00681-9000

Keywords: modular design, outcome-based education, embedded system education

The average American interacts with as many as 100 embedded systems per day. This number continues to grow as newer technologies are developed. This growth denotes the relevance of embedded systems in our lives and highlights the importance of providing a good education in this area. Currently, universities offer courses on embedded system design using different types of teaching methodologies. Well-designed course teaching methodologies cover not only aspect related to embedded system architecture but also on the design process. This research focuses on the development of a new teaching methodology using as a base contemporary design techniques such as modular design and educational frameworks such as outcome-based education (OBE).

We hypothesized that an OBE-based laboratory with a teaching methodology based on a modular design approach shall foster the incorporation of contemporary design skills, aided by progressive lab experiments and module design. These should provide a focus on modularity and how to build embedded systems from an initial idea (necessity), passing through design considerations (module and system design), to a final conception (functional prototype).

To evaluate the hypothesis, an OBE framework was used to structure the laboratory. This framework aims at aligning course content, pedagogical methods, and assessment methods to develop a well-structured lab. The first step in the restructuration was defining the laboratory content. The proposed content was designed following the current Curriculum Guidelines for Undergraduate Degree Programs in Computer Engineering, social & industrial expectations, and the current departmental focus for the computer engineering program. At the end of the process, the content and targeted design skills were summarized in a series of learning objectives to be met by students.

The OBE framework suggests the establishment of pedagogical methods to guide the teaching and learning process. In this phase, a modular design approach was introduced in the laboratory experience through a set of progressive lab experiments and educational modules. The progression of experiments was structured to use in each new unit the abilities learned in the previous experiment. The lab provides eight experiments, each organized in four dedicated sections: objectives, lecture, basic exercises and complementary task.

The educational modules were developed to fulfill the technical objectives of each experiment. A total of six different modules were designed for the entire set of experiments. Some of the modules are used in more than one experiment. Each module was designed to provide students with an example of how electronic modules are structured including functional diagrams, schematics, board design, and software usage guidelines. Modules can then be combined among them with the target microcontroller unit (MCU) to develop embedded applications.

The OBE also includes assessment methods to validate the methodology and assess how well students meet the learning objectives. The assessment methods developed in this project include a set of pre- and post-tests given to the students in each experiment. These tests are aimed at quantifying the prior knowledge students bring into the lab and what knowledge they gained after completing each experiment. As a part of the assessment process, each test was subjected to a validation process to determine the item difficulty, discrimination, and reliability. Also, a learning gain factor was determined for each experiment based on the results obtained in the pre- and post-tests. The validation methodology compares the general lab performance, in terms of test and lab exercises scores. Two groups of students were studied, a control and an experimental group, using an unpaired t-statistic. The control group corresponded to students who took the class with the previous methodology and the experimental group is formed by the students taking the class with the proposed methodology.

Finally, the alignment between the content, methods, and assessments will be carried out through the creation of a student profile. This profile will allow identifying the mastering level revealed by each student in each learning objective and how each activity in the methodology and assessment are related to these objectives.

Currently, the data recollection process for the control group was completed and the data for the experimental group is in process. Preliminary results obtained from the control group show a maximum learning gain factor of 42.6% and shows a trend to create their prototypes from scratch without subdividing them in modules. We expect to improve the gain factor results for the experimental group and we also expect that the t-statistic will show a better performance on a modular design for this group.